Journal of Power Sources 194 (2009) 824–829

Contents lists available at ScienceDirect

Journal of Power Sources

journal homepage: www.elsevier.com/locate/jpowsour

Short communication

Carbon-supported Pd catalysts: Influences of nanostructure on their catalytic performances for borohydride electrochemical oxidation

Jun Qiang Yang, Bin Hong Liu*, Song Wu

Dept. of Material Science and Engineering, Zhejiang University, Hangzhou 310027, PR China

ARTICLE INFO

Article history:
Received 14 May 2009
Received in revised form 12 June 2009
Accepted 12 June 2009
Available online 21 June 2009

Keywords:
Carbon nanotubes
Palladium
Catalyst
Borohydride
Hydrogen evolution

ABSTRACT

In the present work, a Pd catalyst supported on multiwalled carbon nanotubes (MWCNTs) is successfully synthesized and its property as the anode material for borohydride oxidation is investigated. Compared with other carbon-supported Pd catalysts, the Pd/MWCNT catalyst exhibits improved polarization properties due to its smaller Pd particles dispersing homogeneously on carbon nanotubes. The hydrogen evolution behavior on the Pd/activated carbon sample is found to be very sensitive to the concentrations of NaOH and $NaBH_4$ in the solution. On the other hand, borohydride oxidation on Pd/carbon black and Pd/MWCNT displays reaction mechanisms near the 4e stoichiometry. It is thus supposed that the primary direct borohydride oxidation on Pd may be a 4e reaction. The simultaneous electro-oxidation of adsorbed hydrogen occurs conditionally, depending on its relative activity with the direct oxidation of BH_4^-.

1. Introduction

Great changes in global environment due to the devastating use of fossil fuels have urged worldwide efforts in developing clean and efficient renewable energy systems. Fuel cells are promising solutions to environmental issues due to their high energy conversion efficiency and zero-emission by use of hydrogen for power generation. However, their commercialization is now greatly impeded by prohibitive costs and the lack of a hydrogen infrastructure. The direct fuel cells are thus being developed to circumvent the problem of hydrogen storage and supply. The direct borohydride fuel cell (DBFC) is advantageous over hydrocarbon-based direct fuel cells due to its higher energy and power densities, less toxicity and good performance [1–4].

In recent years, efforts have been devoted to develop anode and cathode catalysts [5–10], modify electrode and cell structure [11–13] and improve stack properties of DBFC [14,15]. Consequently, the performances of DBFCs have been significantly enhanced. It was reported recently that a power density as high as 1.5 W cm^{-2} was achieved at 65 °C in a $NaBH_4$–H_2O_2 fuel cell [15], suggesting that the DBFC is very promising as the direct fuel cell. On the other hand, some fundamental problems remain unsettled, especially with respect to hydrogen evolution accompanying with the electrochemical reactions and its relation with the reaction mechanism of borohydride oxidation. In our previous studies, we found that different anode materials showed varied reaction stoichiometries as follows [6]:

$$BH_4^- + xOH^- = BO_2^- + (x-2)H_2O + (4-x/2)H_2 + xe \quad (1)$$

For example, a 4e reaction was observed on Ni electrodes, while those on Pd or Pt electrodes were found to be more complicated. The relation of hydrogen evolution vs. current on a Pd catalyst was highly dependent on the concentration of borohydride, for which the mechanism is still unclear. To achieve a better control of catalyst property, it is necessary to find out all influencing factors and understand the underlying mechanisms. Thus in this work, we prepared a Pd catalyst supported on multiwalled carbon nanotubes (MWCNTs) and compared its property with other two Pd catalysts supported on different carbon materials in order to study the effects of Pd nanostructure on its performance for borohydride oxidation. The different properties shown by these Pd catalysts helped us to elucidate the reaction mechanism and acquire a better understanding of borohydride electro-oxidation.

2. Experimental details

Three Pd catalysts were studied in this work: Pd 10 wt% supported on activated carbon (Wako Chemicals, Japan), Pd 10 wt% on Vulcan XC-72 (E-TEK, USA) and Pd 10 wt% on multiwalled carbon nanotubes (home made). The Pd 10 wt%/MWCNT catalyst was prepared as follows: the as-received carbon nanotube powder was first treated by boiling in concentrated HNO_3 for 3 h to remove possible impurities, and then washed by deionized water until pH became higher than 6, and finally dried in a vacuum oven at 353 K. The

* Corresponding author. Tel.: +86 571 87951770; fax: +86 571 87951770.
E-mail address: liubh@zju.edu.cn (B.H. Liu).

0378-7753/$ – see front matter © 2009 Elsevier B.V. All rights reserved.
doi:10.1016/j.jpowsour.2009.06.034

Pd deposition on MWCNT was initiated by dispersing 250 mg pretreated carbon nanotube power in 150 ml deionized water under ultrasonic agitation, followed by adding pre-dissolved sodium citrate and $PdCl_2$ with a mole ratio of 8:1 into the mixture. The solution was then reduced by adding diluted $NaBH_4$ solution in a slow rate. After 3 h for a sufficient reduction, the Pd-deposited powder was then separated from the solution and washed by deionized water at least three times and dried in the vacuum oven at 353 K.

The electrodes were prepared by first mixing 40 mg Pd/C powder with a certain amount of diluted Teflon emulsion to form a paste, then spreading the mixture on a nickel foam of 1 cm^2 (from ABC Materials Ltd, Shanghai), and then sandwiching it using a stainless steel net and finally pressing the electrode to the form.

The electrochemical tests were carried out at ambient temperature in a three-electrode system consisting of three compartments for the working, counter and reference electrode respectively. The compartment for the working electrode was separated from the other two by Nafion N117 membrane. The distance between the working electrode and the counter electrode was 4.5 cm and the same for the distance between the working electrode and reference electrode. The working electrode compartment was also sealed to measure hydrogen evolution during electrochemical tests. An AB_2-type metal hydride electrode was used as the counter electrode and a Hg/HgO electrode as the reference electrode. Polarization properties of the electrodes were measured on a Kikusui PFX2011 battery testing system.

X-ray diffraction (XRD) and high-resolution transmission electron microscopy (HRTEM) analyses were performed to characterize the nanostructures of the carbon-supported Pd catalysts. The XRD analyses were carried out on PANalytical X'Pert PRO with Cu Kα radiation and the HRTEM analyses were on CM200UT of Philips. Co., Netherlands.

3. Results

3.1. Nanostructure characterization of the carbon-supported Pd catalysts

In this study, three carbon-supported Pd catalysts were employed to investigate the effects of catalyst nanostructure on its performance for borohydride oxidation. They were Pd 10 wt% on activated carbon (Pd/AC), Pd 10 wt% on carbon black Vulcan XC-72 (Pd/CB) and Pd 10 wt% on multiwalled carbon nanotubes (Pd/MWCNT). Fig. 1 shows the XRD patterns of three catalysts, along with that of the bare MWCNT for comparison. It could be observed that the Pd/AC sample demonstrates apparent Pd peaks of (1 1 1), (2 0 0), (2 2 0), and (3 1 1), suggesting that the catalyst nanoparticles were well crystallized. In contrast, the Pd/CB sample only reveals a very weak and indiscernible peak centered at 40° (2θ), implying a nanocrystalline or disordered structure of particles. By comparing the XRD pattern of Pd/MWCNT with that of the bare MWCNT sample, we could observe a broader peak around 40° (2θ) that overlaps with a small and sharp peak from MWCNT, indicating that the nanoparticles in Pd/MWCNT were amorphous.

Fig. 2 shows the HRTEM observations on three Pd catalysts. The photos illustrate that Pd particles in the Pd/AC sample are smaller than 5 nm but most of them coalesce and aggregate together, resulting in inhomogeneous distribution on the carbon support. On the other hand, Pd particles in Pd/CB are of 2–3 nm and disperse discretely and homogenously on the carbon substrate. Also from Fig. 2, it can be well observed that Pd particles in Pd/MWCNT are the smallest among three samples. These particles with a size of about 2 nm are scattered uniformly on carbon nanotubes.

Combining the analysis results of XRD and HETEM, we can summarize that the Pd/AC sample had larger crystalline Pd particles with less uniform distribution, while Pd/CB and Pd/MWCNT had smaller and discretely scattered amorphous Pd particles. Moreover, due to its unique structure, MWCNTs were supposed to possess the largest specific surface area among three carbon materials. Therefore, MWCNT-supported Pd catalyst constituted an ideal nanostructure for electrochemical catalysis.

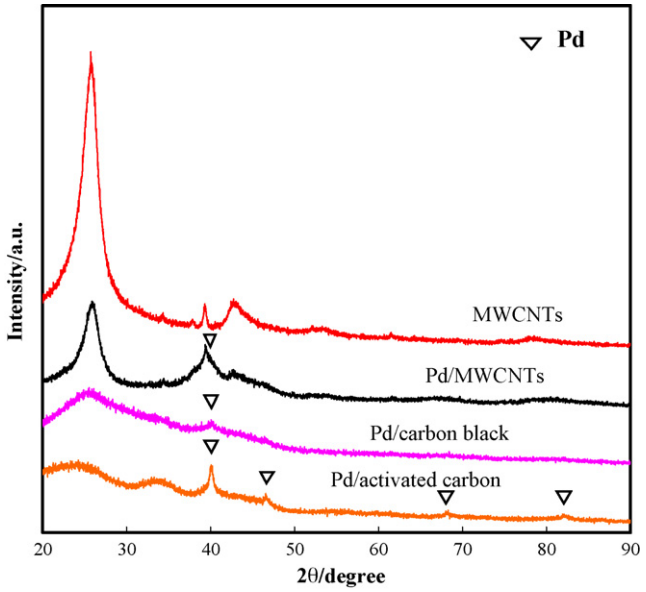

Fig. 1. XRD patterns of the carbon-supported Pd catalysts and the multiwalled carbon nanotube sample.

3.2. Polarization properties of the carbon-supported Pd catalysts

The open-circuit potentials of three electrodes are listed in Table 1. Compared with Pd/AC showing a potential of −0.89 V vs. SHE, Pd/CB and Pd/MWCNT demonstrated more negative potentials of −0.93 V and −0.98 V vs. SHE respectively in a 0.5 M $NaBH_4$–6 M NaOH solution. Fig. 3(a) and (b) shows the polarization properties of three Pd electrodes in different solutions. It can be seen that the Pd/MWCNT electrode reveals the smallest overpotential, followed by the Pd/CB electrode. On the other hand, the Pd/AC electrode has the largest polarization among the three. This result is well consistent with the observed nanostructures of the catalysts. The carbon nanotubes with diameters of around 5 nm owned the largest surface area among three carbon materials. Its crystalline structure and metallic nature also made it a better electric conductor than the other two amorphous carbon materials [16]. In addition, Pd particles in Pd/MWCNT appeared to be the smallest. All these justify for the best polarization property of Pd/MWCNT. In contrast, the largest size and the least uniform dispersion of Pd particles in the Pd/AC sample yielded the largest overpotential. Therefore with more negative open-circuit potential and decreased overpotential, Pd/MWCNT is considered as a better catalyst for borohydride oxidation.

Table 1
Open-circuit potentials (OCP) demonstrated by three carbon-supported Pd catalysts in a 0.5 M $NaBH_4$–6 M NaOH solution at 288 K.

Electrodes	OCP (V vs. SHE)
Pd 10 wt% on activated carbon (Pd/AC)	−0.89
Pd 10 wt% on carbon black (Pd/CB)	−0.93
Pd 10 wt% on multiwalled carbon nanotubes (Pd/MWCNT)	−0.98

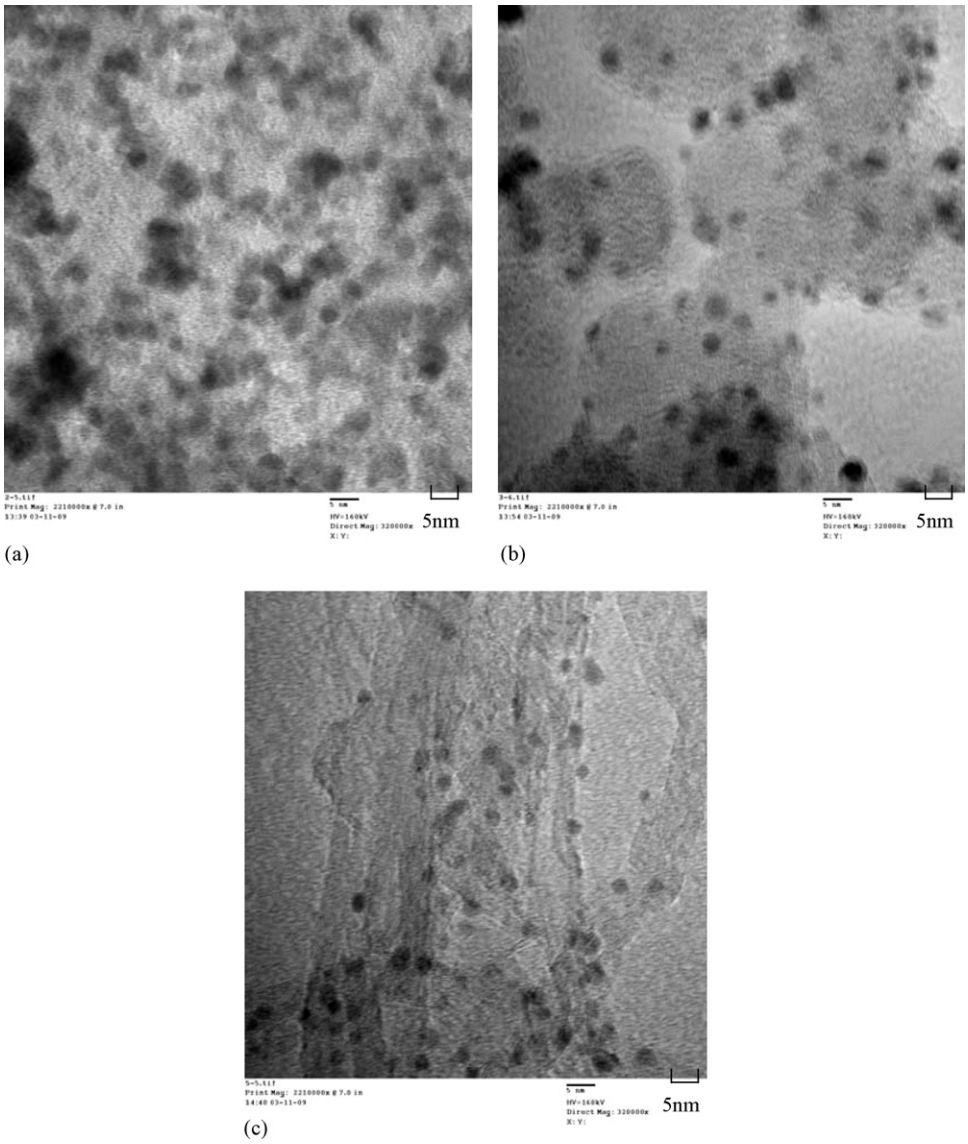

Fig. 2. HRTEM images showing the nanostructures of three carbon-supported Pd catalysts. (a) Pd/activated carbon; (b) Pd/carbon black; (c) Pd/MWCNT.

3.3. Hydrogen evolution

In our previous study [6], borohydride oxidation on the carbon-supported Pd catalyst (Pd 10 wt% on activated carbon) displayed a variable reaction mechanism. The fuel efficiency strongly depended on the borohydride concentration. It could reach 75% at low borohydride concentrations, but decreased with increasing borohydride concentration when the NaOH concentration was fixed at 6 M. In this study, both the concentrations of NaOH and $NaBH_4$ were varied to examine their effects on reaction mechanisms. As shown in Fig. 4(a) and (b), the relation of hydrogen evolution with current for the Pd/AC electrode is significantly influenced by both the concentrations of NaOH and $NaBH_4$. When the borohydride concentration was fixed at 1 M, increasing the NaOH concentration resulted in the decrease of hydrogen evolution. On the other hand, when the NaOH concentration was fixed at 6 M, increasing the $NaBH_4$ concentration led to the increase of hydrogen evolution. If Fig. 4(a) and (b) are combined into Fig. 4(c), it could be perceived that the slope drawn in the plot for $NaBH_4$:NaOH = 1 M:3 M is almost the same as that for $NaBH_4$:NaOH = 2 M:6 M. Similarly, $NaBH_4$:NaOH = 1 M:4 M and 1.5 M:6 M demonstrate analogous relation. These results strongly suggest that the concentration ratio of $NaBH_4$:NaOH might be the controlling factor in deciding reaction mechanism. Fig. 4(c) clearly shows that the higher the ratio of OH^-/BH_4^-, the less the hydrogen is evolved. This result confirms that there was a competition between the electrochemical reaction and the hydrogen evolution reaction. A high ratio of OH^-/BH_4^- reduced the fraction of hydrogen evolution.

Although the apparent coulombic number on Pd/AC showed strong OH^-/BH_4^- dependence, the number of OH^-/BH_4^- mole ratio was not exactly equal to the observed coulombic number. For example, a 4e relation was achieved when OH^-/BH_4^- was 2, or a 6e relation was achieved when OH^-/BH^- was 5. One possible reason for the shift is that the surface concentrations of reaction species might be different from the bulk ones.

On the other hand, when Pd/CB and Pd/MWCNT were used, hydrogen evolution was found to be less influenced by the concentrations of NaOH or $NaBH_4$ in the solution. As shown in Fig. 5(a) and (b), when NaOH or $NaBH_4$ concentration was largely varied, the slope of hydrogen evolution vs. current was changed very little and became approaching to the 4e reaction stoichiometry (OH^-/BH_4^- = 1:1 usually induced exceptions).

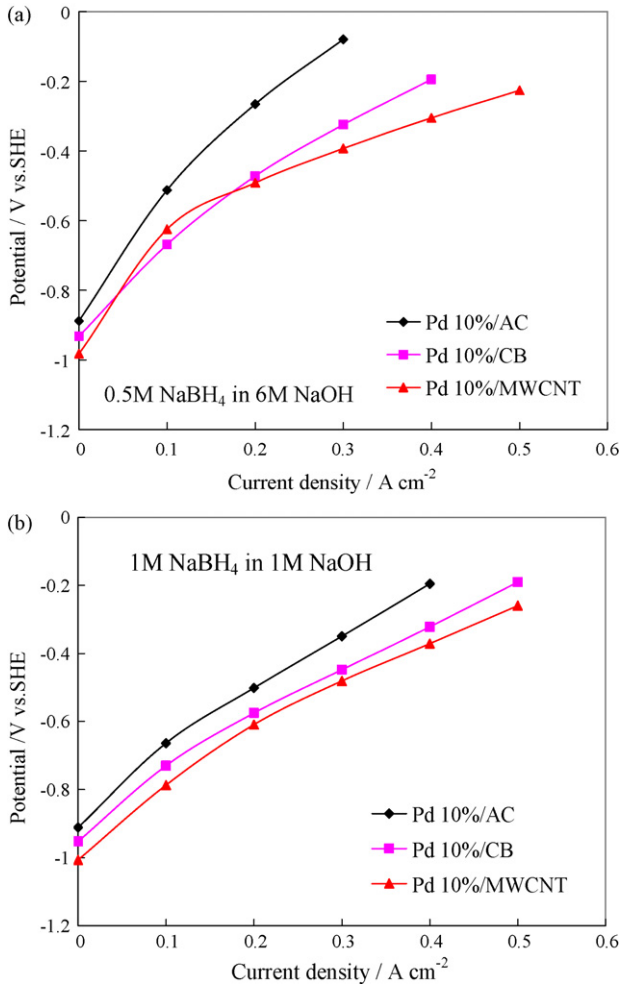

Fig. 3. Comparison of the polarization properties for three carbon-supported Pd catalyst (Pd 4 mg cm^{-2}) at 288 K: (a) in 0.5 M $NaBH_4$–6 M NaOH; (b) in 1.0 M $NaBH_4$–1 M NaOH.

Three Pd catalysts demonstrated different hydrogen evolution behaviors, indicating that the electro-oxidation of borohydride was significantly influenced by the nanostructures of the Pd catalysts. It is expected that elucidation of the hidden mechanism of this phenomenon could help us to grasp the catalytic mechanism of Pd and get a deeper understanding of borohydride electro-oxidation. A detailed discussion on these issues is made in the next section.

4. Discussion

Combining all the results obtained in our previous studies [6] and in this research, we suppose that on the Pd electrodes the primary electrochemical reaction starting from BH_4^- (including derivatives such as BH_3OH^-) might be a 4e reaction as follows:

$$BH_4^- + 4OH^- = BO_2^- + 2H_2O + 4H_{ad} + 4e \quad (2)$$

This deduction is mainly based on the observations on Pd/CB and Pd/MWCNT electrodes which demonstrated mostly the 4e or near 4e relations. Fig. 5 also implies that this reaction is less dependent on OH^-/BH_4^- in the solution.

H_{ad} from the above reaction (or from the chemical hydrolysis reaction) might be further oxidized through following reaction:

$$H_{ad} + OH^- = H_2O + e \quad (3)$$

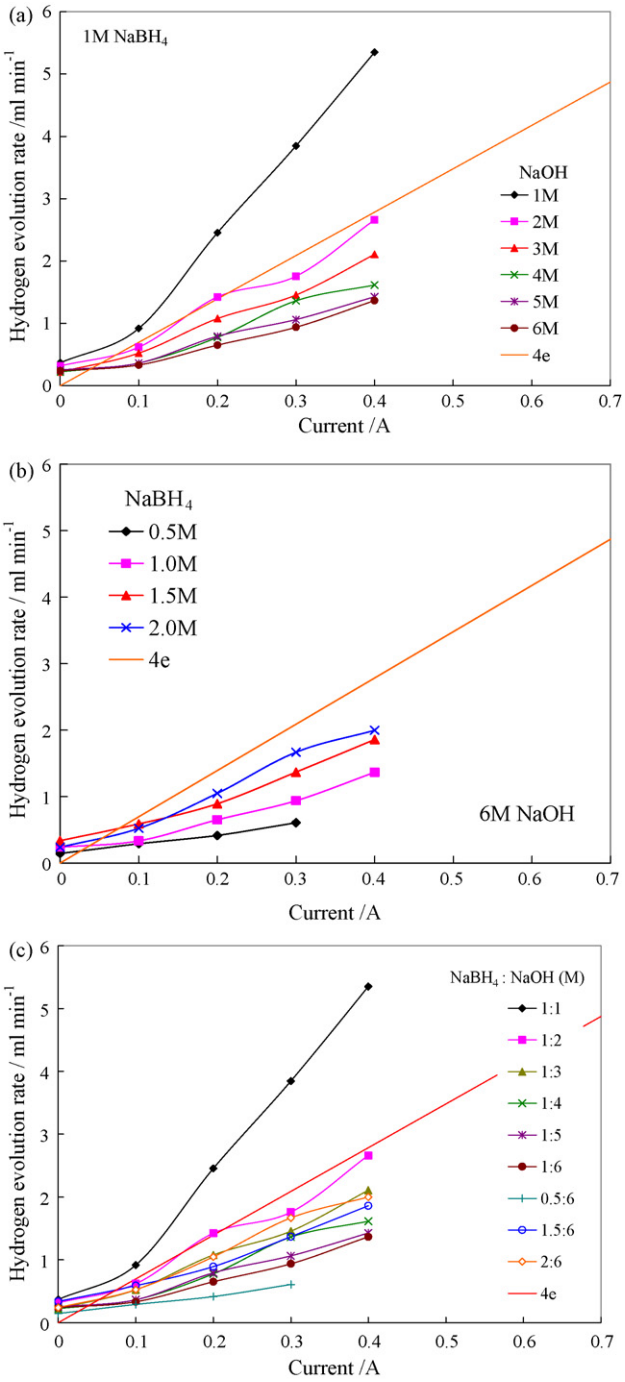

Fig. 4. Relation of hydrogen evolution rate vs. current influenced by the concentrations of NaOH and $NaBH_4$ in the solution for the Pd/AC electrode at 288 K. (a) Change with the NaOH concentration; (b) change with the $NaBH_4$ concentration; (c) change with the ratio of $NaBH_4$:NaOH.

Or two H_{ad} combine to form hydrogen gas and evolve out:

$$H_{ad} + H_{ad} = H_2 \quad (4)$$

The concurrence of reactions (2) and (3) is presumably determined by their relative activities. Fig. 6 illustrates two possible cases concerning the relative activities of two oxidation species. In the case (a), the polarization curve of the H_{ad} oxidation situates slightly above that of the direct BH_4^- oxidation, the concurrence of two reactions is possible as the combination of i_{BH} (current contributed from direct electrochemical oxidation of BH_4^- or derivatives) and i_H (current contributed from electrochemical oxidation of adsorbed

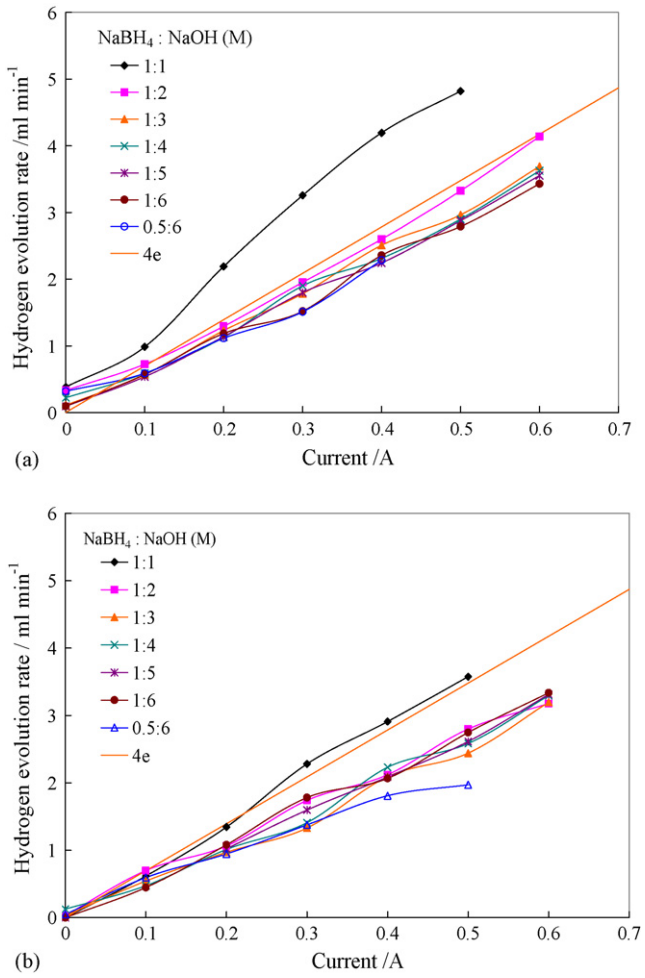

Fig. 5. Hydrogen evolution vs. current for the Pd/CB and Pd/MWCNT electrode at 288 K. (a) Pd/carbon black; (b) Pd/MWCNT.

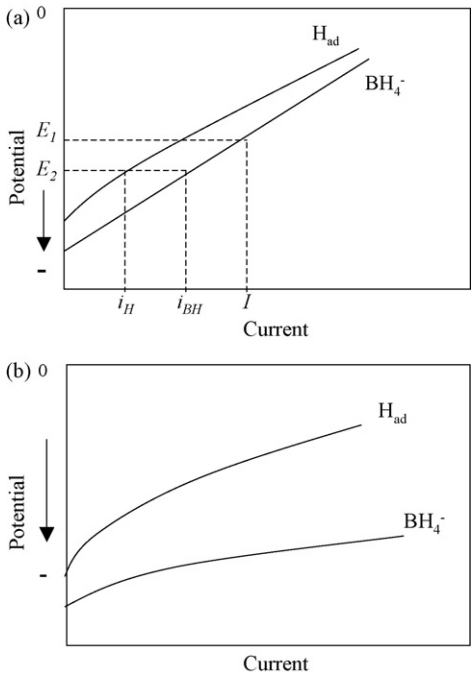

Fig. 6. (a and b) Schematic illustrations of two cases with respect to the relative activities of the direct BH_4^- oxidation and the adsorbed atomic hydrogen on a Pd electrode.

hydrogen) would lead to a reduced overpotential compared with a single current I from BH_4^- (the interaction between i_{BH} and i_H is omitted for simplicity). In the case (b), two polarization curves are apart from each other, the BH_4^- oxidation shows much smaller overpotentials than that of H_{ad}, resulting in a low probability of the H_{ad} oxidation. Based on this postulation, we can explain that at lower BH_4^- concentrations, larger polarizations of BH_4^- oxidation make the simultaneous oxidation of H_{ad} possible. As a result, the apparent fuel efficiency is increased. With increasing the BH_4^- concentration, the relative activities of two species would change due to the enhancement of the BH_4^- side. Consequently, reaction (2) becomes dominating on the electrode.

Furthermore, as both reactions (2) and (3) require OH^-, the OH^- concentration is another important factor in deciding reaction pathways. A high OH^- concentration is apparently necessary for H_{ad} oxidation because otherwise the combination of H_{ad} will be more facile. As a result, the ratio of OH^- to BH_4^- in the solution largely decides the probability of reaction (3) and therefore the fuel efficiency.

Besides the concentrations of NaOH or $NaBH_4$ in the solution, the relative activities of reactions (2) and (3) also depend on the electrode catalyst. When the catalyst nanostructure was improved such as from Pd/AC to Pd/CB and Pd/MWCNT, it appears that reaction (2) became much more active than reaction (3), as in the case (b) of Fig. 6. As a result, the direct borohydride oxidation became prevailing on the electrode. The shifts of open-circuit potentials to more negative side for the Pd/CB and Pd/MWCNT electrodes provide evidences for the BH_4^- domination, as the open-circuit potential is the mixing potential of reactions (2) and (3) (the calculated theoretical potential of reaction (2) is −1.654 V vs. SHE and that of reaction (3) is −0.828 V vs. SHE). In addition, as can be seen from Fig. 7, the polarization properties of Pd/CB and Pd/MWCNT electrodes at $NaBH_4$:NaOH = 0.5 M:6 M were greatly enhanced, even better than those of Pd/AC at higher $NaBH_4$ concentrations. It is supposed that the probability of H_{ad} oxidation was largely reduced due to the prevailing BH_4^- oxidation on these electrodes. In this case, the observed coulombic numbers which were a little larger than 4e suggest only small contributions from oxidation of adsorbed hydrogen.

If the mechanism proposed above is justified, i.e. the current is the sum of i_{BH} from reaction (2) and i_H from reaction (3), and then the total current could be written as:

$$I = i_{BH} + i_H$$

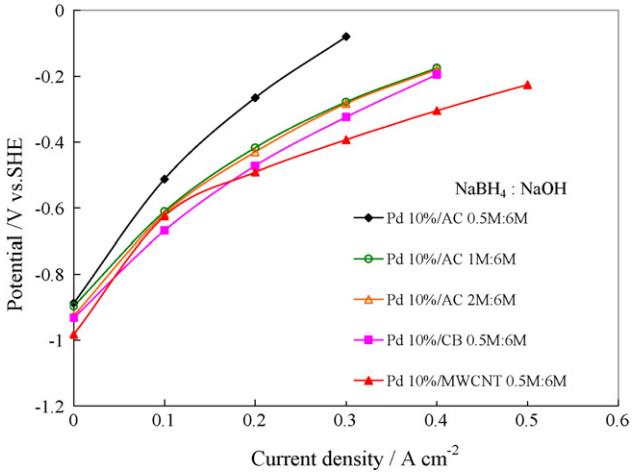

Fig. 7. Electrode polarizations influenced by the concentrations in solution and the catalyst material (288 K).

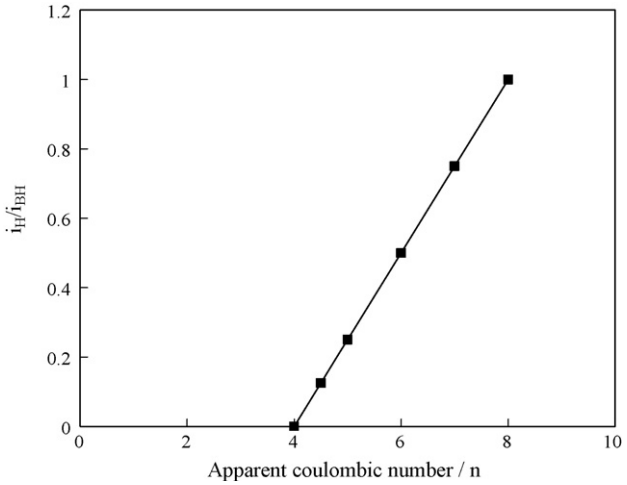

Fig. 8. Relation of i_H/i_{BH} with the observed apparent coulombic number according to the proposed reaction mechanism.

i_{BH} is accompanied with hydrogen generation and i_H consumes hydrogen. Thus if there is no chemically generated hydrogen, the net hydrogen gas generation rate should be:

$$V_H = \frac{22400 \times 60}{2F}(i_{BH} - i_H) \quad (\mathrm{ml\,min^{-1}},\ F:\ \text{Faraday constant})$$

From the observed relation of V_H with I, i_{BH} and i_H can be calculated as:

$$i_{BH} = \frac{1}{2}\left(I + \frac{2FV_H}{22400 \times 60}\right), \qquad i_H = \frac{1}{2}\left(I - \frac{2FV_H}{22400 \times 60}\right)$$

Fig. 8 shows the relation of i_H/i_{BH} with the observed apparent columbic number. For example, if the observed relation for V_H with I is a 4.5e relation, the i_H/i_{BH} is 1/8. The 8e relation corresponds to $i_H/i_{BH} = 1$.

From the above deduction, it could be understood that the varied hydrogen evolution behaviors observed on the Pd electrodes originated from the competition between two oxidation species. As a result, all the factors influencing their relative activities affected the observed apparent fuel efficiency. It seems that the key point for obtaining high fuel efficiency on Pd electrodes is how to facilitate the simultaneous oxidization of the adsorbed hydrogen atom. The above results and discussion clearly show that the manipulation of nanostructure for Pd catalyst is very important. Apart from their varied particle size and dispersion, structural differences with these Pd catalysts may partially account for the changed catalytic performances. It is supposed that the particles with well-crystallized structure in Pd/AC gave anisotropy surfaces possibly showing different catalytic activities towards BH_4^- and H_{ad} oxidation, allowing for the variable reaction pathways. In contrast, disordered particles in Pd/CB and Pd/MWCNT presented isotropy surfaces and thus demonstrated the relatively simple mechanism.

5. Conclusions

Three carbon-supported Pd electrodes with different kinds of carbon materials and nanostructures were used for electrochemical oxidation of borohydride. The electrodes using Pd supported on multiwalled carbon nanotubes demonstrated improved polarization properties due to smaller size and better dispersion of catalyst particles. The relation of hydrogen evolution vs. current on the Pd/activated carbon sample was found to be dependent on the concentrations of NaOH and $NaBH_4$. Hydrogen evolution was depressed and fuel efficiency was increased by increasing the NaOH concentration and decreasing $NaBH_4$ concentration. Moreover, it seems that the concentration ratio of OH^-/BH_4^- was the real determining factor for fuel efficiency. On the other hand, borohydride oxidation on Pd/carbon black and Pd/MWCNT displayed near 4e reaction mechanisms. It is thus supposed that the primary electrochemical oxidation of BH_4^- on the Pd catalysts might be a 4e reaction. The secondary electrochemical oxidation of adsorbed hydrogen is possible but restricted by its relative activity with the direct oxidation of BH_4^-. The catalyst nanostructure and concentration ratio of NaOH and $NaBH_4$ were found to be important factors influencing the relative activities of two species.

Acknowledgements

The authors would thank Dr. Fu Liu in Dept. of Material Sci. and Eng., Zhejiang University for generously providing the multiwalled carbon nanotube sample. This work was supported by the National Hi-tech Program of 863 under the contract no. 2007AA05Z144.

References

[1] S.C. Amendola, P. Onnerud, P.T. Kelly, P.J. Petillo, S.L. Sharp-Goldman, M. Binder, J. Power Sources 84 (1999) 130–133.
[2] C.P. de Leon, F.C. Walsh, D. Pletcher, D.J. Browning, J.B. Lakeman, J. Power Sources 155 (2006) 172–181.
[3] J.H. Wee, J. Power Sources 155 (2006) 329–339.
[4] U.B. Demirci, J. Power Sources 169 (2007) 239–246.
[5] Z.P. Li, B.H. Liu, K. Arai, S. Suda, J. Electrochem. Soc. 150 (2003) A868–A872.
[6] B.H. Liu, Z.P. Li, S. Suda, Electrochim. Acta 49 (2004) 3097–3105.
[7] R.X. Feng, H. Dong, Y.D. Yang, X.P. Ai, Y.L. Cao, H.X. Yang, Electrochem. Commun. 7 (2005) 449–452.
[8] M.H. Atwan, C.L.B. Macdonald, D.O. Northwood, E.L. Gyenge, J. Power Sources 158 (2006) 36–44.
[9] H. Cheng, H. Scott, J. Electroanal. Chem. 596 (2006) 117–123.
[10] J. Ma, J. Wang, Y.N. Liu, J. Power Sources 172 (2007) 220–224.
[11] K.T. Park, U.H. Jung, S.U. Jeong, S.H. Kim, J. Power Sources 162 (2006) 192–197.
[12] H. Cheng, K. Scott, K.V. Lovell, J.A. Horsfall, S.C. Waring, J. Membr. Sci. 288 (2007) 168–174.
[13] R. Jamard, A. Latour, J. Salomon, P. Capron, A. Martinent-Beaumont, J. Power Sources 176 (2008) 287–292.
[14] G.H. Miley, N. Luo, J. Mather, R. Burton, G. Hawkins, L. Gu, E. Byrd, R. Gimlin, P.J. Shrestha, G. Benavides, J. Laystrom, D. Carroll, J. Power Sources 165 (2007) 509–516.
[15] N. Luo, G.H. Miley, K.J. Kim, R. Burton, X. Huang, J. Power Sources 185 (2008) 685–690.
[16] A.L. Dicks, J. Power Sources 156 (2006) 128–141.